Analysis of the incoherent intermediate scattering function in the framework of the idealized mode-coupling theory: A Monte Carlo study for polymer melts

Jörg Baschnagel
Institut für Physik, Johannes-Gutenberg Universität, Staudinger Weg 7, D-55099 Mainz, Germany
(Received 8 March 1993)

In this Monte Carlo simulation, we calculate the incoherent intermediate scattering function $\phi_q^s(t)$ for a three-dimensional dense polymer melt after having made long relaxation runs in order to eliminate the history of the cooling procedure sufficiently. This function shows the signature of a two-step process in the temperature interval $T \in [0.16, 0.21]$ (the temperature is measured in units of an energy parameter introduced in the Hamiltonian of the model) whose time evolution was quantitatively analyzed in the framework of the idealized mode-coupling theory (MCT) within the β-relaxation regime. As a result of this analysis the temperature interval splits into high- and low-temperature parts. In the high-temperature part ($T \geq 0.19$), the idealized theory accounts very well for the decay of $\phi_q^s(t)$ over about three decades in time, whereas $\phi_q^s(t)$ relaxes much faster than the idealized MCT anticipates in the low-temperature region ($T < 0.19$). Since this discrepancy between the idealized MCT and the simulation data can qualitatively be rationalized by taking hopping processes into account, we try to estimate the critical temperature T_c from the fits with the idealized MCT, yielding $T_c \approx 0.150$.

I. INTRODUCTION AND OVERVIEW

Glasses are materials that possess an amorphous short-range order comparable to that of a liquid.[1,2] There is thus no sharp distinction between the fluid and the glassy state on structural grounds, but they differ from each other in the typical values of the structural relaxation time, which might be measured by the shear viscosity η, for instance. Whereas the viscosity of a liquid in its ordinary state usually varies between $\eta \approx 10^{-2}$ and 10^{-1} poise, corresponding to a time scale of picoseconds,[3,4] its value increases over many orders of magnitude when the liquid is more and more undercooled. If the viscosity enters the range of $\eta \geq 10^{13}$ poise, the associated structural relaxation time τ becomes macroscopic, i.e., $\tau \approx 10^2$ s or larger. Therefore the temperature, corresponding to $\eta = 10^{13}$ poise, has operationally been defined as the glass transition temperature T_g and a lot of experimental work[5,6] has been invested in order to elucidate the mechanism of structural relaxation in the viscosity region close to and below $\eta = 10^{13}$ poise, which means that one was primarily concerned with the time window $\tau \in [10^{-6}, 10^3]$ s. However, in the past years the interest has also been focused on the regime around $\eta \approx 10^2$ poise, corresponding to a time scale of nanoseconds, where the plot of the viscosity versus temperature typically changes slope for all fragile glass formers,[7,8] due to the development of the mode-coupling theory (MCT) for the structural glass transition.[9,10]

The central result of this theory is the assertion that there exists a critical temperature T_c well above T_g, where the dynamics of the undercooled fluid qualitatively changes from a behavior, which is typical of an ordinary liquid to one which can be considered glasslike.[9–11] In its original idealized version[9,11] the MCT predicts that for all temperatures $T \leq T_c$ the particles of the fluid are permanently trapped in the cages, which are formed by their neighbors[3,4] without any chance to escape so that density fluctuations no longer decay totally, but level off at a constant value, which can be interpreted as a measure of the solidity of the glassy material. Above the critical temperature density fluctuations always decay to zero, which means that the cages only succeed in localizing the captured particle for a finite time before it finds a path to escape. Therefore, the critical temperature itself is the distinguished point where a spontaneous breaking of ergodicity occurs.[9,12] However, the idealized version of the MCT overestimates the tendency of the liquid to freeze, since the discussion of the fluid dynamics is exclusively based on the cage effect[9] and thus ignores the ability of a particle to leave its cage by an activated hopping process. These hopping processes compete with the localization property of the cages, and it is a major result of the extended version of the MCT (Refs. 10 and 13) that the inclusion of the hopping processes restores ergodicity for all temperatures around the critical point. Although the idealized MCT is thus incomplete from a physical point of view it has initiated both many experiments[14–23] and computer simulations.[24–30] Therefore, the validity of the idealized theory could be tested with very different techniques for a variety of liquids, ranging from computer generated simple liquids,[24,28] lattice gases,[27] or polymers[29] to real experimental glass formers such as organic liquids,[18] ionic salts,[19,20] colloidal suspensions,[14] migrogels,[21] polymers,[22] or even proteins.[23] Although the structure of most of the experimental systems is considerably more complicated than that of a simple liquid for which the basic equations of the MCT were derived an impressive quantitative agreement between the theory and the experiment is partly found.[14,20,21]

Especially in the research on the dynamical behavior of undercooled polymer melts many of the features of the idealized MCT were discovered.[22,31,32] In comparison to these experiments, computer simulations are still lacking behind. Presumably one reason for this fact might be that the relaxation time of a polymer in a melt exceeds the typical relaxation time of a simple liquid already in its normal state by many orders of magnitude so that it is an exacting problem to equilibrate the melt properly from a computational point of view. The problem becomes the more severe the closer the calorimetric glass transition is approached because the structural relaxation time then tends to increase beyond any bound. Since the mode-coupling approach to the glass transition is an equilibrium theory, any reasonable attempt to check its predictions must guarantee that the system has been relaxed long enough so that the signature of the mode-coupling processes might not be blurred by nonequilibrium effects.[27] In the case of polymer melts it is, therefore, not advisable to work with an atomistically detailed model. A lot of valuable computer time would then be spent to relax all the microscopic degrees of freedom such as the bond-length, the bond-angles or the torsional angles,[33] from which one does not know if their explicit consideration is really indispensable to generate the dynamical features that the MCT describes. However, an unprejudiced look at the variety of fragile glass formers, mentioned above, which certainly differ extensively in their chemical structure, but all show many aspects of the MCT, rather suggests that it is not necessary to include all microscopic details in the simulation. Therefore, one can also work with a simplified coarse-grained model, preferably a lattice model, which only retains the essential properties of a polymer and has the advantage of allowing a very efficient simulation by the Monte Carlo technique. Then it becomes possible to follow the dynamical evolution of the system over a considerably larger time interval than in an atomistically realistic off-lattice simulation and to obtain good statistics, which might be necessary if one wants to attempt a quantitative comparison with the MCT.

In this spirit we use the three-dimensional version of the bond-fluctuation method[34–36] combined with a suitable model Hamiltonian, which generates the glassy behavior of the polymer melt. Some basic properties of this model were investigated in two previous studies,[41,37,38] where we tried to understand how the choice of the cooling rate influences the temperature variation of typical quantities, such as the mean bond-length or the radius of gyration, and the structure of the melt, when it is continuously cooled down from the liquid to the glassy state, and to what extent the underlying lattice of the simulation emerges in the results. These first studies were indispensable in order to obtain valuable insight in the relaxation behavior of the model, in order to discover the interesting temperature region, where mode-coupling effects might be expected and in order to work out the details of the calculation and properties of the collective structure factor whose knowledge is a necessary input of the MCT. Starting with this information, we determined the incoherent intermediate scattering function and tried to analyze its decay quantitatively in the framework of the idealized MCT. The present paper is devoted to the discussion of the results. It is organized as follows. Section II will supply some details about our model, the simulation method and the important question of equilibration. In Sec. III we review the theoretical background of our analysis, whereas Sec. IV presents and discusses our results. The final section, Sec. V, summarizes the main conclusions and gives a short overview how we want to proceed.

II. MODEL AND SIMULATION METHOD

In this Monte Carlo simulation we use the three-dimensional bond-fluctuation model[34–36] in which the polymers are represented by mutually avoiding walks and self-avoiding walks[39](SAW's) on a simple-cubic lattice and each monomer occupies a whole unit cell of the lattice. In order to introduce the temperature in this *a priori* athermal model we energetically favor long-bond vectors[37,38] so that a competition between the energetic and topological constraints of the chains is created, which prevents crystallization, if the density of the melt is suitably chosen. A possible choice is $\phi = 0.5\bar{3}$,[37,38] resulting from $\phi = 8NP/L^3$, where the degree of polymerization N, the number of polymers per simulation box P and the length of one side of the simulation box L are $N = 10$, $P = 180$, and $L = 30$, respectively. In total, the simulation box thus contains 1800 monomers. In order to improve the statistics still further, 16 independent configurations of this system were run so that the total statistics of the data to be presented are based on 28 800 monomers.

As a starting point of this simulation we used the configurations of our previous study, which we had generated during a cooling process from $T = \infty$ to $T = 0.05 = \beta_{\max}^{-1}$,[40] with the slowest cooling rate of $\Gamma_Q = 4 \times 10^{-7}$ MCS's^{-1},[37] which means that we reach the smallest $T = 0.05$ in 2.5×10^6 Monte Carlo steps (MCS's).

In order to get a feeling of how the abstract Monte Carlo time unit can be related to conventional units of time one has to take into account that a monomer of the bond–fluctuation model stands for a group of chemical monomers of a real chain. Since this group typically contains about five chemical monomers for simple polymers, such as polyethylene,[42,43] for instance, the motion of a monomer in the bond-fluctuation model should correspond to bond reorientational jumps in the torsional potential of a real polymer whose relaxation time is of the order of 10^{-11} s. Although this identification, 1 MCS $\approx 10^{-11}$ s, is only a rough estimate, which may depend upon the choice of the model Hamiltonian,[38] it reveals that a simulation over 10^6–10^7 MCS's corresponds to a time scale, which is comparable to that of a neutron-scattering experiment.[22]

Even for the above quoted smallest cooling rate of our previous study the melt falls out of equilibrium in a narrow temperature range around $T \approx 0.2$. Since the MCT assumes thermal equilibrium of the fluid and the criti-

cal temperature of the theory seems to lie in the range below $T = 0.2$ (see Sec. IV) one has to allow the melt to relax in order to eliminate the history of the cooling process as much as possible. To this end, long relaxation runs of 4×10^6 MCS's were made at every temperature of the interval $T \in [0.16, 0.21]$ before the incoherent intermediate scattering function was calculated. Although even this amount of time is smaller than the Rouse time τ_R[44] and is thus too short to equilibrate the melt on the length scale of the end-to-end distance of the polymers smaller length scales, such as that of a bond-vector or of the persistence length,[44] which are of prime importance in this simulation, have already relaxed sufficiently. Without these long relaxation runs the signature of the two-step process, which the incoherent intermediate scattering function $\phi_q^s(t)$ exhibits in the above cited temperature interval (see Sec. IV) and which is the necessary precondition to justify an interpretation in the framework of the MCT, might be blurred or even lost. This effect is exemplified in Fig. 1, which compares the shape of $\phi_q^s(t)$ recorded after a relaxation time of 4×10^6 MCS's (crosses in Fig. 1) with that after an equilibration period of 6×10^3 MCS's (diamonds in Fig. 1) at same temperature of $T = 0.16$. Whereas the data used in the further analysis clearly show a two-step process, this essential prediction of the MCT is nearly completely hidden by nonequilibrium effects in the curve with the small relaxation time. If one tried to describe the decay of $\phi_q^s(t)$ quantitatively by the asymptotic expansions of the β-relaxation regime [see (6) and (7)] the results of the fit would be entirely wrong. For instance, the α-relaxation time would turn out to be too small by more than an order of magnitude, as a glance at Fig. 1 shows. This example proves how crucial a sufficient relaxation time is for a meaningful application of the MCT.

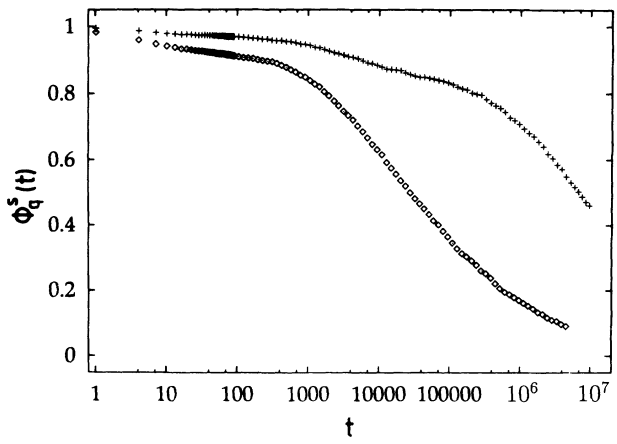

FIG. 1. Comparison of the shape of $\phi_q^s(t)$ at the external temperature $T = 0.16$ after the melt has relaxed for 4×10^6 MCS's (crosses) and 6×10^3 MCS's (diamonds). Note that the curve with the smaller relaxation time has much more decayed than the other and that the two-step process is barely visible. This indicates that the external temperature is considerably smaller than the internal temperature of the melt as a consequence of insufficient relaxation.

III. THEORETICAL BACKGROUND AND FITTING PROCEDURE

As mentioned in the Introduction, the idealized MCT elaborates the dynamical implications of the physical picture that the motion of every fluid particle is always confined by the surrounding particles, which try to enclose it in its cage. The trapped particle rattles in this cage until it finds a way to pass over a distance of typically one nearest neighbor to a new environment. The overall motion of the particles leads to local density fluctuations around the average density of the system. If the fluid is in its normal nonundercooled state the particles can easily change their cages so that the density-density correlation function will rapidly decay. However, if the fluid freezes in a glassy state the particles will remain in their cages for a long, eventually unmeasurably long, time so that a certain residue of density-density correlations could persist.[9] These physical considerations suggest choosing the (normalized) density-density correlation function, i.e., the density correlator $\phi_q(t)$, as the appropriate coarse-grained variable to signal the onset of the glass transition, which has the additional advantage that it is directly accessible in experiments as the intermediate coherent scattering function.[9] Using the Mori-Zwanzig projection operator formalism[3,4] it is possible to derive an equation of motion for the density correlator or for other correlators such as the tagged particle density-density correlation function.[9] The tagged particle correlator $\phi_q^s(t)$ or the incoherent intermediate scattering function, as it is called in scattering experiments, is of particular importance in this simulation, since the analysis of the next section is based on it. For this quantity the Mori-Zwanzig formalism produces the following equation of motion[9]

$$\frac{\partial^2}{\partial t^2}\phi_q^s(t) + \nu_q^s \frac{\partial}{\partial t}\phi_q^s(t) + \left(\Omega_q^s\right)^2 \phi_q^s(t) + \left(\Omega_q^s\right)^2 \int_0^t m_q^s(t-t') \frac{\partial}{\partial t'}\phi_q^s(t')\, dt' = 0, \quad (1)$$

whereby ν_q^s is the coefficient of a white-noise term, which does not influence the interesting long-time behavior of $\phi_q^s(t)$, Ω_q^s is the characteristic frequency, which defines the time scale t_0 of the microscopic motion, where mode-coupling effects are not yet dominant and $m_q^s(t)$ is a memory kernel, which links the time evolution of $\phi_q^s(t)$ to the history of its motion. The essence of the mode-coupling approximation is to expand this memory kernel in products of $\phi_q(t)$ with $\phi_q^s(t)$.[9] The simplest possible expansion adopts the following form[9]

$$m_q^s(t) = \frac{1}{V} \sum_{\mathbf{k}+\mathbf{p}=\mathbf{q}} V^s(\mathbf{q},\mathbf{p},\mathbf{k})\, \phi_p^s(t) \phi_k(t). \quad (2)$$

In (2) V in the prefactor of the sum stands for the volume of the system and the expansion coefficients $V^s(\mathbf{q},\mathbf{p},\mathbf{k})$ are called the coupling constants of the theory. They depend upon the density and the temperature of the

system through the static structure factor and related quantities.[9] Since the density does not change during a Monte Carlo simulation in the canonical ensemble the temperature is the only relevant control parameter, which can drive the melt along a path in the space $\mathcal{K}$ of all coupling constants from the liquid side, where the coupling constants are small, to the strong-coupling region of the glassy states. A major result of the MCT is that the weak and the strong-coupling region are separated by a critical surface S_c, where the central equation (1) possesses a solution with a nonzero long-time limit, which is called nonergodicity parameter

$$f_q^s(T_c) =: f_q^{sc}. \tag{3}$$

Although the MCT has been derived for simple liquids, a test based on a polymer model does not only seem to be justified by the numerous experimental examples in which polymer data were used to confirm the predictions of the idealized MCT,[22,31,32] but it can also be rationalized by the theoretical argument that the existence of the critical surface S_c in $\mathcal{K}$ is a result of the asymptotic solution of (1), which is independent of the details of coupling vertices in (2) and thus of the precise nature of the interparticle interaction. This interaction will certainly modify the topology of the coupling space. It will influence the path followed by the system during the cooling process and determine the point of impact on the critical surface so that the critical temperature and the exponent parameter λ, to be defined below, depend upon the interaction potential of the fluid particles. However, no new singularities are introduced by it.[9] Due to this property of the solution of (1) it was supposed that the applicability of the MCT is not exclusively confined to simple liquids, but that the theory approximately grasps the essential universal features, which are responsible for the glass transition of all fragile glass formers. In order to exemplify this theoretical conjecture one should therefore try to look for the signature of the MCT in systems, which are much more complicated than simple liquids, such as in a dense polymer melt of absolutely monodisperse and linear chains, for instance, whose interactions with each other (hard-core interaction) are much simpler than in experimental systems so that subtle contributions to the dynamical behavior due to the specific chemical properties can be excluded.

One of these universal results of the MCT concerns the form that the tagged particle correlator has to adopt in the β-relaxation regime close to the critical temperature[9,13]

$$\phi_q^s(t) = f_q^{sc} + h_q^s G(t). \tag{4}$$

This so-called reduction theorem implies that $\phi_q^s(t)$ consists of a time-independent term given by the nonergodicity parameter [see (3)] and a time dependent term in which the whole wave vector dependence is carried by the critical amplitude h_q^s, whereas the dynamical evolution of the fluid in the β-regime and its temperature dependence is exclusively determined by the correlator $G(t)$ for *all* length scales in the system. In the framework of the idealized MCT the β-correlator $G(t)$ obeys a one parameter scaling law

$$G(t) = c_\varepsilon g(t/t_\varepsilon), \tag{5}$$

where ε, the so-called separation parameter, denotes the reduced distance to the critical temperature, i.e., $\varepsilon := (T_c - T)/T_c$, and the scaling function $g(t/t_\varepsilon)$ can be expanded on the liquid side ($\varepsilon < 0$) in the following way:[45]

$$g(t/t_\varepsilon) = (t_\varepsilon/t)^a - A_1(t/t_\varepsilon)^a + A_2(t/t_\varepsilon)^{3a} - A_3(t/t_\varepsilon)^{5a} \quad \text{for} \quad t_0 \ll t \le t_\varepsilon \tag{6}$$

and

$$g(t/t_\varepsilon) = -B(t/t_\varepsilon)^b + (B_1/B)(t_\varepsilon/t)^{2b} \quad \text{for} \quad t_\varepsilon \le t \le \tau. \tag{7}$$

The short-time part of this expansion (6), which is governed by the exponent a ($a \in]0, 0.5[$), describes the relaxation of the fluid particle in its cage, whereas the long-time part (7) physically corresponds to the escape of the particle from it and thus to the onset of overall structural relaxation, i.e., to the α process.[9] The first term of (7) is usually called the von Schweidler law, and it introduces a new exponent b ($b \in]0, 1]$), which is related to the critical exponent a by the exponent parameter $\lambda \equiv \lambda(T_c)$ through the following transcendental equation:

$$\lambda = \frac{\Gamma(1+b)^2}{\Gamma(1+2b)} = \frac{\Gamma(1-a)^2}{\Gamma(1-2a)}, \tag{8}$$

where Γ stands for the gamma function and λ can adopt all values from the interval $\lambda \in [0.5, 1[$. In Ref. 45 it was shown that the short- and the long-time expansion of $g(t/t_\varepsilon)$ match with an accuracy of about 1% on the intermediate time scale t_ε so that one can use them to construct the full scaling function. In addition to the prefactor c_ε of the β correlator in (5) the two time scale t_ε and τ, which are the relevant scales for the β and the α process, respectively, also depend critically upon temperature by virtue of the following expressions

$$c_\varepsilon = \sqrt{|\varepsilon|}, \tag{9}$$

$$t_\varepsilon = t_0 |\varepsilon|^{-1/2a} = t_0 \left(\frac{T - T_c}{T_c}\right)^{-1/2a}, \tag{10}$$

and

$$\tau = t_0 |\varepsilon|^{-\gamma} = t_0 \left(\frac{T - T_c}{T_c}\right)^{-\gamma}. \tag{11}$$

In (11) the new exponent γ is fully determined by the exponents a and b: $\gamma = 1/2a + 1/2b$. If one knows the temperature dependence of the microscopic time scale t_0, one can then use Eqs. (10) and (11) to determine the critical temperature. The time scale t_0 corresponds to the transient short-time decay of the correlator in a time regime where mode-coupling effects are not yet dominant and can thus be obtained from an independent microscopic theory for the system under consideration. Since short polymers in a dense melt often exhibit a Rouse-like behavior,[46,47] we try to describe the initial decay of $\phi_q^s(t)$

by the respective expansion of the Rouse model, which is valid for times that are both larger than a crossover time $t_{\rm cross}$, below which the microscopic details of the model affect the dynamics of the monomers, and much smaller than the longest relaxation time of the chain, i.e., the Rouse time τ_R

$$\phi_q^s(t) \approx \exp\left[-q^2\langle b_{npc}^2\rangle_{npc}\sqrt{t/t_0}\right] \quad \text{for} \quad t_{\rm cross} < t \ll \tau_R, \tag{12}$$

where $\langle b_{npc}^2\rangle_{npc}$ stands for the mean-squared bondlength averaged over all monomers n, polymers p and configurations c.

Having gathered all this theoretical information, one can now try to fit the simulation data in the time window of the β process close to the critical temperature with the asymptotic expressions (4), (5), (6), and (7). *A priori*, these equations contain four unknown parameters: the nonergodicity parameter f_q^{sc}, the total prefactor of the scaling function $h_q^s c_\epsilon$, the time scale of the β process t_ϵ, and the critical exponent a.

In the framework of the idealized MCT one could have also chosen the von Schweidler exponent b or the exponent parameter λ as the fourth fit parameter instead of the critical exponent a, since they are related to each other by the transcendental equation (8). In fact, the exponent parameter was used to fit the decay of the coherent intermediate scattering function in a recent dynamic light scattering study of concentrated migrogel solutions, and it was shown that the idealized theory accurately describes the experimental data over up to eight decades in time[21]. However, it is *a priori* not clear to what extent a fluid will show the signature of the idealized MCT, since this version of the theory overestimates the freezing tendency of the liquid due to the neglect of hopping processes which are characterized by a temperature-dependent frequency δ.[13] This frequency δ introduces a natural scale ε_0 for the separation parameter, given by

$$|\varepsilon_0| = (\delta t_0)^{\frac{2a}{1+2a}}, \tag{13}$$

which separates the liquid region, where the idealized MCT can be applied, from the region in the immediate vicinity around the critical temperature, where the hopping effects dominate the β dynamics. Therefore the idealized theory is expected to work on the liquid side in a temperature window between some value $\varepsilon_{\rm min}$, below which the asymptotic expressions (4), (5), (6), and (7) no longer hold, and ε_0.[13] Another result of this extended version of the MCT is that the critical exponent a always stays the same, irrespective of the size of δ, whereas the von Schweidler exponent b may change from the value, which is tightly coupled to a by (8), to a universal one of 1/2, if the temperature crosses the border ε_0, provided that the exponent parameter is larger than $\pi/4$, i.e., $\lambda > 0.785$. Since we did not know *a priori* how important hopping effects are for the system under consideration, we have therefore chosen the critical exponent a as the fourth fit parameter instead of b or λ, as was also done in Ref. 20.

The actual fitting procedure now consists of two steps: First, one tries to describe the decay of $\phi_q^s(t)$ at every temperature in the relevant temperature window by adjusting all four parameters simultaneously until one discovers a pair of values for f_q^{sc} and a for which it is possible to fit all temperatures satisfactorily. This first trial and error step also serves to assess the error bars for the nonergodicity parameter and the critical exponent, which the MCT requires to be temperature independent. Fixing the found values of f_q^{sc} and a, the second step consists in repeating the whole fitting procedure with two open parameters, $h_q^s c_\epsilon$ and t_ϵ, for all temperatures in order to obtain their temperature dependence. The results of this second step together with the value of a can then be used to derive the critical temperature with the help of (9) and (10).

Since this analysis based on the expansion of the scaling function does not simultaneously yield the time scale τ of the α process, it has to be determined by a separate fit, for instance with the empirical Kohlrausch-Williams-Watts formula,[1]

$$\phi_q^s(t) = f_q^{sc}\exp\left[-(t/\tau_K)^{\beta_K}\right], \tag{14}$$

where the temperature-independent Kohlrausch exponent β_K typically ranges between 0.3 and 0.8 for structural glasses. Although it is not possible to obtain the Kohlrausch law as a solution of the idealized mode-coupling theory for the α-process generally,[9,32] it implies the time-temperature superposition principle,[1,9] which is in turn a major result of the idealized MCT, and a comparison of the Kohlrausch law with the numerical solution of the mode-coupling equation for the α process has shown that one can use it as a convenient fit formula for the time window following the von Schweidler law, i.e., for times $t \geq \tau$. The application of the Kohlrausch law to the simulation data proceeds in exactly the same two steps, as explained above. Using the result for the nonergodicity parameter from the analysis with the idealized MCT the first step serves to determine the value and the errors of the Kohlrausch exponent β_K, whereas one keeps it fixed for all temperatures in the second step in order to extract the temperature dependence of the α time scale τ_K and thus the critical temperature by virtue of (11). Since the application of the Kohlrausch law assumes the validity of the time-temperature superposition principle, and this principle states that all times in the α-relaxation regime share the same temperature dependence we have used the time value $\tau_{1/2}$, where $\phi_q^s(\tau_{1/2})$ becomes 1/2, in addition to τ_K in order to test Eq. (11). The same strategy to estimate the α-time scale was also adopted in Ref. 21. From a theoretical point of view one can rationalize this choice by the fact that the von Schweidler part of the scaling function (7) concatenates the β- with the α-relaxation regime, and thus all data points, which fall in this part, such as $\tau_{1/2}$, have to obey both the scaling law of the β and of the α process.

IV. ANALYSIS OF THE INCOHERENT INTERMEDIATE SCATTERING FUNCTION

The whole analysis is based on the time evolution of the incoherent intermediate scattering function $\phi_q^s(t)$, which

was determined by the following formula during the simulation

$$\phi_q^s(t) = \frac{1}{NP}\sum_{n=1}^{NP}[\langle\cos\{\mathbf{q}\cdot[\mathbf{r}_{nc}(t)-\mathbf{r}_{nc}(0)]\}\rangle_c]_q, \quad (15)$$

where $\mathbf{r}_{nc}(t)$ is the vector to the center of gravity of the nth monomer in configuration c at time t, $\langle\cdots\rangle_c$ represents the average over all independent configurations and the symbol $[\cdots]_q$ stands for the lattice analogue of a spherical average in the continuous reciprocal space.[38] This function was calculated for six q values, namely, $q = 1.65, 2.1, 2.53, 2.92, 3.0, 3.2$, distributed around the maximum of the collective static structure factor, which lies at $q = 2.92$,[38] and six different temperatures ranging from $T = 0.21$ to 0.16.[40] For the three higher temperatures $T = 0.19, 0.20, 0.21$ we monitored the time evolution of $\phi_q^s(t)$ over a period of 5×10^6 MCS's, whereas we simulated twice as long for the remaining lower temperatures $T = 0.16, 0.17, 0.18$. Therefore, the overall length of our simulation covers six to seven decades in time, a length that is comparable to that of a very recent lattice gas simulation.[27]

A. Qualitative aspects of the simulation data

Figures 2 and 3 compile the simulation results for all studied q values at the lowest and at the highest temperature, i.e., at $T = 0.16$ and $T = 0.21$, respectively. With increasing q value one can see that a two-step process starts to emerge at $T = 0.21$ and that it becomes stronger developed at $T = 0.16$. The detection of the two-step process in this polymer melt, where the first step cannot stem from the fast relaxation of side groups, is therefore a strong indication that mode-coupling effects might play a prominent role for the time evolution of the tagged particle correlator in the chosen temperature interval. Another qualitative feature of Figs. 2 and 3 is the fact that the intensity of $\phi_q^s(t)$ decreases with increasing

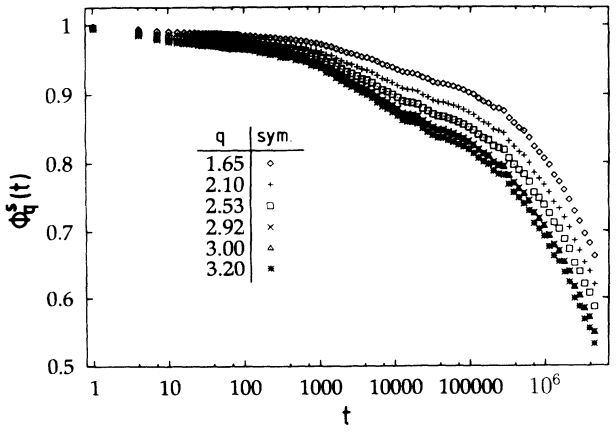

FIG. 2. Simulation data of $\phi_q^s(t)$ for the six q values of this simulation, i.e., $q = 1.65$ (diamonds), $q = 2.1$ (crosses), $q = 2.53$ (squares), $q = 2.92$ (times), $q = 3.0$ (triangles), and $q = 3.2$ (stars) at $T = 0.16$. $q = 2.92$ corresponds to position of the maximum of the collective static structure factor.

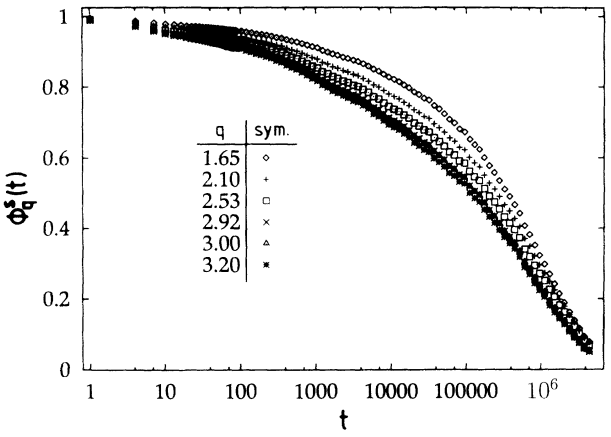

FIG. 3. Simulation data of $\phi_q^s(t)$ for the six q values of this simulation at $T = 0.21$ using the same choice as in Fig. 2.

q values in the time regime of the two-step process so that the first step becomes more visible. Since the first step corresponds to the critical decay of the correlator to the nonergodicity parameter f_q^{sc} a decrease of f_q^{sc} would mean that the initial decay of $\phi_q^s(t)$ in the β-regime gets more pronounced. In fact, the MCT predicts that f_q^{sc} decreases with rising q values according to[9]

$$f_q^{sc} = \exp\left[-q^2 r_{sc}^2\right]. \quad (16)$$

In (16) the length r_{sc} measures the available space that a particle has at the critical temperature. Therefore, the loss of intensity of $\phi_q^s(t)$ with rising q values qualitatively agrees with the behavior required by the theory. Motivated by the formula (16), one can ask if it is not possible to map the whole time dependence of the correlator $\phi_q^s(t)$ on the mean square displacement of a monomer by the ansatz

$$\phi_q^s(t) = \exp\{-q^2\langle[\mathbf{r}_{nc}(t)-\mathbf{r}_{nc}(0)]^2\rangle_{nc}\}. \quad (17)$$

Such a description for $\phi_q^s(t)$ naturally appears in the analytical treatment of polymer dynamics if one assumes very long chains with a Gaussian shape.[44] Therefore, polymer theory anticipates that the interplay of the time and q value dependence of the tagged particle correlator is less complicated than the MCT predicts. If this different conjecture was correct, the ratio $-\ln\phi_q^s(t)/q^2$ should no longer be dependent upon q for all times. In order to test (17) we chose one time from the regime of the scale t_0, $t = 150$ MCS's, and three time values from the regime of the β and the α process, i.e., $t = 1005, 50\,794, 5\,000\,100$ MCS's. Figures 4 and 5 present the results of this analysis for $T = 0.21$ and $T = 0.16$, respectively. At both temperatures one can see that the ratio $-\ln\phi_q^s(t)/q^2$ is more weakly dependent upon q than the Gaussian approximation predicts and that the difference between the simulation data and the Gaussian approximation becomes the more pronounced the larger the considered time value is. Therefore, the functional relationship between $\phi_q^s(t)$ and q is more sophisticated than (17) assumes, which justifies to try other concepts such as the mode-coupling approach.

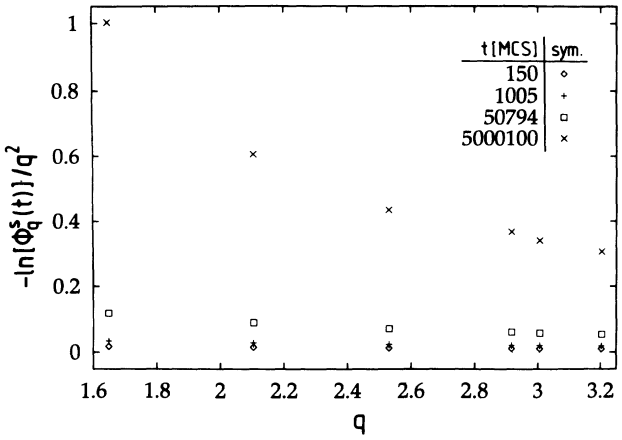

FIG. 4. Plot of $-\ln\phi_q^s(t)/q^2$, vs q at $T = 0.21$ for four different time values, i.e., $t = 150$ MCS's (diamonds), $t = 1005$ MCS's (crosses), $t = 50\,794$ MCS's (squares), and $t = 5\,000\,100$ MCS's (times) in order to test (17).

B. Quantitative analysis

The six figures 6–11, referring to each of the studied temperatures individually, contain the details of the line shape analysis of $\phi_q^s(t)$, which is represented as a solid line in all plots so that the agreement between the fitting formulas and the simulation data can better be estimated.

For all of the considered temperatures one can see that the short time expansion of $\phi_q^s(t)$ within the Rouse model [see (12)] describes the initial decay of the correlator very well in a time window, which increases with decreasing temperature. Whereas the validity of the Rouse model is confined to about one decade (i.e., $t \in [60, 1600]$ MCS's), for $T = 0.21$ the window of its applicability considerably expands in the directions of both smaller and larger times the lower the temperature becomes, resulting in an accurate description over about 2.5 decades (i.e., $t \in [10, 8000]$ MCS's) at the lowest temperature $T = 0.16$. Hence the microscopic time scale t_0 strongly depends upon temperature and this contribution has to be removed from the results of the fitting by the MCT in order to work out

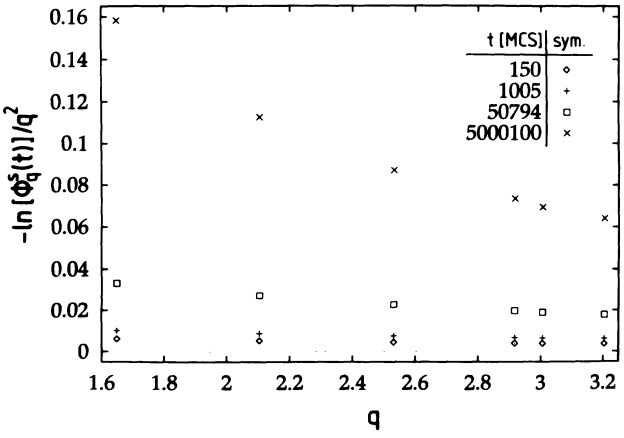

FIG. 5. Plot of $-\ln\phi_q^s(t)/q^2$ vs q at $T = 0.16$ for the same time values and the same choices as in Fig. 4.

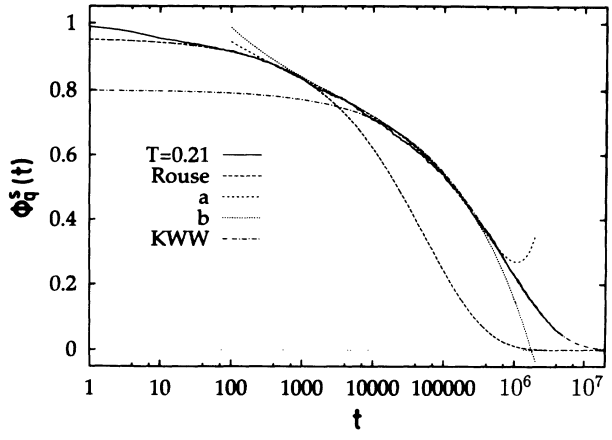

FIG. 6. Comparison of the simulation data (solid line) and various fitting formulas at $T = 0.21$. The short-time expansion of Rouse model (12) and the Kohlrausch law (14) are represented by a dashed line with long dashes and by a dashed-dotted line, respectively. The dashed line with the short heavy dashes corresponds to short-time expansion of the MCT (6), whereas the dotted line refers to the long-time part of the scaling function (7).

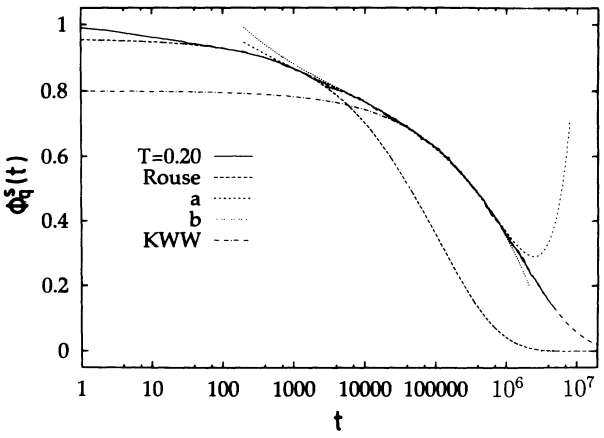

FIG. 7. Comparison of the simulation data with the same fitting formulas and the same choice for the types of the lines as in Fig. 6 at $T = 0.20$.

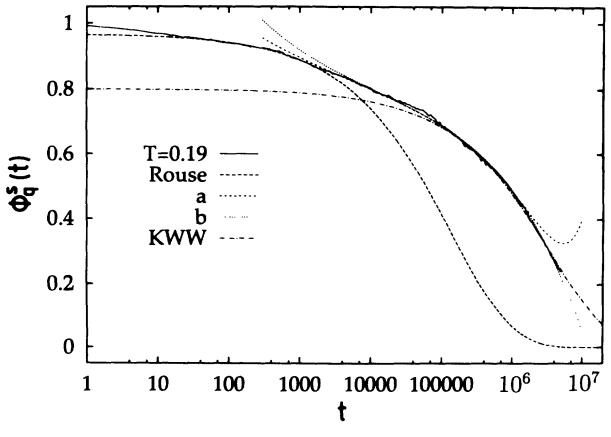

FIG. 8. Comparison of the simulation data with the same fitting formulas and the same choice for the types of the lines as in Fig. 6 at $T = 0.19$.

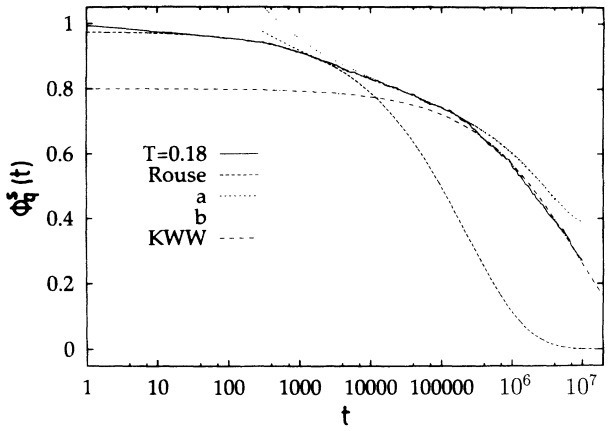

FIG. 9. Comparison of the simulation data with the same fitting formulas and the same choice for the types of the lines as in Fig. 6 at $T = 0.18$.

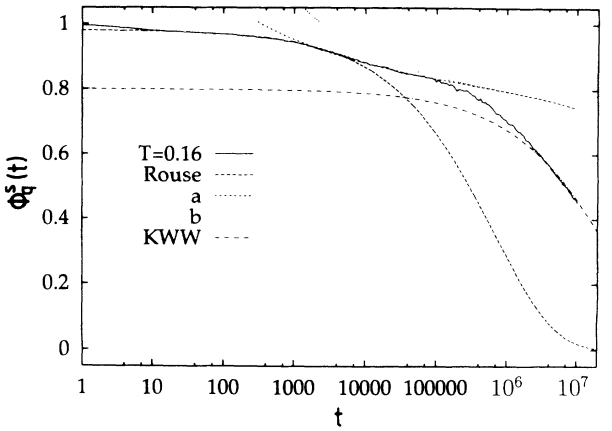

FIG. 11. Comparison of the simulation data with the same fitting formulas and the same choice for the types of the lines as in Fig. 6 at $T = 0.16$.

the linear dependence of the β and the α time scale upon the separation parameter as clearly as possible.

The MCT starts to describe the decay of the tagged particle correlator in the last time regime, where the Rouse model applies to the simulation data, resulting in a very good matching of the Rouse theory and the short-time expansion of the scaling function (6) at all studied temperatures. Although this short-time expansion coincides with the measured curve of $\phi_q^s(t)$ over at least 1.5 decades for all temperatures, a glance at Figs. 6–11 immediately shows that the temperature interval over which the idealized theory can fully account for the major part of the decay of the intermediate scattering function is limited to $T \geq 0.19$. For smaller temperatures the simulation data progressively fall below the prediction of the idealized MCT so that we want to discuss the low-temperature regime $T < 0.19$ separately from the high-temperature one. In the high-temperature region one obtains by the described fit procedure the following results:

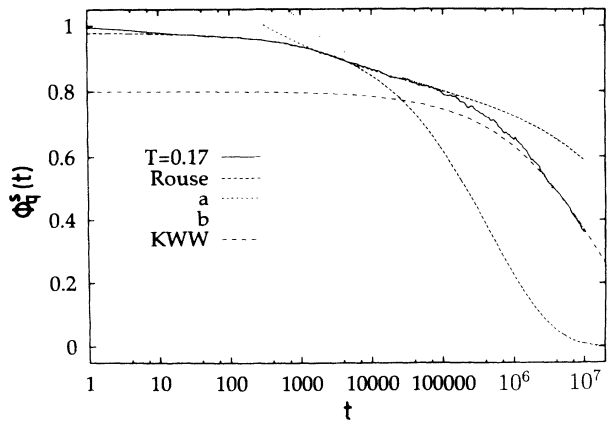

FIG. 10. Comparison of the simulation data with the same fitting formulas and the same choice for the types of the lines as in Fig. 6 at $T = 0.17$.

$$a = 0.239 \pm 0.030, \quad b = 0.370,$$
$$\gamma = 3.443, \quad \lambda = 0.863 \pm 0.052 > \frac{\pi}{4};$$
$$f_q^{sc} = 0.80 \pm 0.03. \tag{18}$$

Figures 6–8 show that these parameters allow to fit the simulation data for $T = 0.21$ over about three decades, reaching from 4×10^2 to 4×10^5 MCS's, whereas the respective time interval slightly extends for the smaller temperatures, ending at 10^6 MCS's for $T = 0.20$ and at 5×10^6 MCS's for $T = 0.19$. Therefore, the outer edge of the interval, where the MCT applies, shifts to about one decade in time which is much stronger than the respective shift of the end of the time interval, where the Rouse theory describes the simulation data, in the same temperature range. This means that the time scale of the β process separates more and more from the microscopic time scale t_0 with decreasing temperature and that the interval where the simulation data are close to the formulas of the reduction theorem increases. This feature qualitatively agrees with the predictions of the idealized MCT for the β regime and has been observed in experiments.[48] Figure 8 also shows how the asymptotic expansions (6) and (7) are tailored so that they can complete each other in order to describe the decay of a correlator as far as possible. Since the extended von Schweidler law (7) diverges faster than (6) for small times the short time part of the scaling function begins to describe the simulation data before (7) catches up with (6) for times $t \propto t_\varepsilon$. If the α and the β process are sufficiently separated the von Schweidler part of the scaling function will continue the fit of the correlator, while (6) departs from it for $t \gg t_\varepsilon$. This qualitative picture only appears for $T = 0.19$, whereas the extended von Schweidler law (7) does not substantially contribute to improve the fit at the higher temperatures. Hence the simulation data show that the α and the β process are not very well separated, and thus the time scale τ of the α process does not expand faster than t_ε in the considered temperature range contrary to the prediction of the idealized theory. This interpretation is also supported by

TABLE I. Values of t_0, $h_q^s c_\epsilon$, t_ϵ, τ_K, and $\tau_{1/2}$ resulting from the fits to $\phi_q^s(t)$ at the different temperatures of this simulation.

T	$t_0 \times 10^{-8}$	$h_q^s c_\epsilon \times 10^2$	$t_\epsilon \times 10^{-4}$	$\tau_K \times 10^{-5}$	$\tau_{1/2} \times 10^{-5}$
0.21	3.004 ± 0.038	6.034 ± 0.803	1.129 ± 0.583	6.360 ± 0.274	1.352
0.20	5.942 ± 0.105	5.791 ± 0.718	2.589 ± 1.239	15.364 ± 1.099	3.420
0.19	8.062 ± 0.217	5.377 ± 0.771	5.603 ± 2.894	36.358 ± 3.227	9.113
0.18	12.617 ± 0.252	4.137 ± 0.130	12.366 ± 6.559	80.802 ± 8.173	16.924
0.17	26.869 ± 0.530	3.591 ± 0.491	53.058 ± 36.346	163.136 ± 22.508	36.691
0.16	37.300 ± 10.445	2.207 ± 1.046	379.768 ± 332.928	313.404 ± 61.156	69.519

the attempt to describe the long-time decay of $\phi_q^s(t)$ by a Kohlrausch law with an exponent $\beta_K = 0.515 \pm 0.020$, resulting from a fit to simulation data in the whole temperature range $T \in [0.16, 0.21]$ while fixing the prefactor in (14) to $f_q^{sc} = 0.8$. Figures 6–8 show that the Kohlrausch law not only successfully continues the fit of the MCT to arbitrarily long times, but it also penetrates the β regime considerably. In fact, the Kohlrausch law starts to describe the decay of $\phi_q^s(t)$ already close to t_ϵ (compare Table I) in this high-temperature range, whereas one would have expected this to happen only for $t \gg t_\epsilon$ according to the idealized theory. Hence the idealized theory certainly overestimates the freezing tendency of polymer melt in this simulation. This fact clearly appears in Figs. 9, 10, and 11 for the temperatures below $T = 0.19$. The more the temperature is reduced and the better the two-step process becomes visible the stronger the formulas 4–7 deviate from the actual simulation data so that only the initial decay of the first step can be adequately fitted by the short-time expansion (6) of the idealized MCT. However, it is possible to rationalize such a result within the extended version of the MCT by introducing a new time scale $\tilde{t}$ below which (6) remains valid, whereas for time values larger than $\tilde{t}$ one has to work with other asymptotic expansions that take the hopping processes into account.[13] Due to the weak separation of the β and the α processes and the deficiency of the idealized theory in the fitting of $\phi_q^s(t)$ below $T = 0.19$ hopping processes seem to have a decisive influence on the relaxation of the tagged particle correlator in this simulation so that it was very important to use a, and not b or λ, as the fourth fit parameter. Whether the inclusion of the hopping term actually succeeds in extending the fit of the idealized theory for $T < 0.19$, is not clear at present and can only be verified if one applies the extended scaling theory to the simulation data. For the time being one can, however, try to extract an estimate for the critical temperature from the data of the fitting procedure by the idealized theory, which are compiled in Table I, using Eqs. (9)–(11). The results are shown Figs. 12, 13, and 14. For the β time scale and the amplitude of the scaling function one clearly obtains a straight line, which yields a critical temperature of $T_c = 0.146^{+0.006}_{-0.008}$ for t_ϵ and of $T_c = 0.153^{+0.005}_{-0.009}$ for $h_q^s c_\epsilon$, respectively. Therefore, the critical temperatures, resulting from the fit with the formulas of the reduction theorem, coincide within the error bars, whereas they do not agree with values derived from the α time scales $\tau_{1/2}$ and τ_K whose temperature variation is compared in Fig. 14. Based on Eq. (11) one would have expected that a plot of $(t_0/\tau)^{1/\gamma}$ versus T should intersect the temperature axis at T_c for both time values if the time-temperature superposition principle applied. However, Fig. 14 shows that only the results in the high-temperature region approximately behave linearly, whereas the curve for both $\tau_{1/2}$ and τ_K starts to bend around $T = 0.18$ and becomes much weaker dependent on temperature than the idealized theory anticipates for $T < 0.18$. If one uses only the high-temperature data to estimate the critical temperature the linear regression gives $T_c = 0.118^{+0.002}_{-0.003}$ for $\tau_{1/2}$ and $T_c = 0.105^{+0.014}_{-0.019}$ for τ_K. Although these two values agree again with each other within the error bars, yielding an average critical temperature of $T_c = 0.112^{+0.008}_{-0.012}$ from the α time

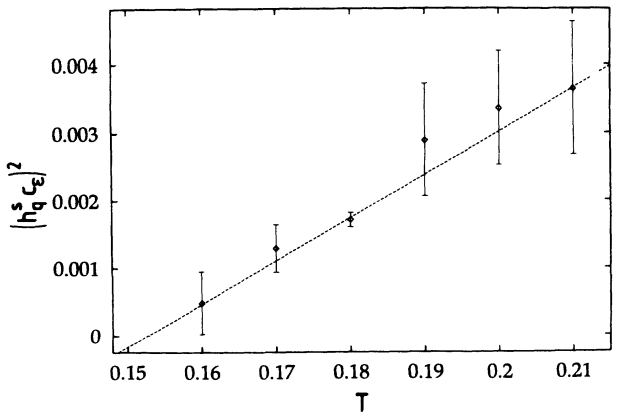

FIG. 12. Plot of $\left(h_q^s c_\epsilon\right)^2$ vs temperature [see (9)]. The diamonds represent the results from Table I, whereas the dashed line is a least-squares fit, yielding a critical temperature of $T_c = 0.153$.

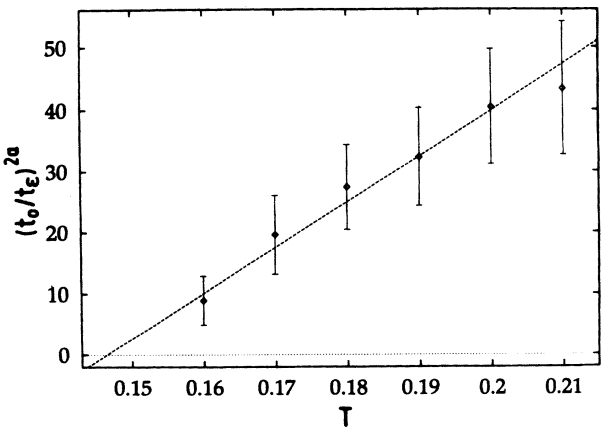

FIG. 13. Plot of $(t_0/t_\epsilon)^{2a}$ vs temperature [see (10)]. The diamonds represent the results from Table I whereas the dashed line is a least-squares fit, yielding a critical temperature of $T_c = 0.146$.

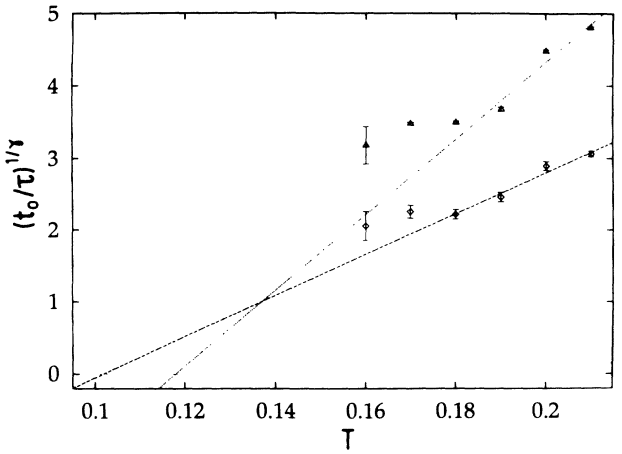

FIG. 14. Plot of $(t_0/\tau)^{1/\gamma}$ vs temperature [see (11)] . The triangles correspond to the times where $\phi_q^s(t)$ adopts a value of 1/2 at the respective temperature, whereas the diamonds represent the results from the Kohlrausch fit. The dotted and the dashed line are the least-squares fits to the temperature interval $T \in [0.19, 0.21]$ for $\tau_{1/2}$ and τ_K, yielding a critical temperature of $T_c = 0.118$ and $T_c = 0.105$, respectively.

scales this average critical temperature is not compatible with the combined result of t_ϵ and $h_q^s c_\epsilon$, which reads $T_c = 0.150^{+0.005}_{-0.009}$. Due to the above-mentioned possible relevance of the hopping term for the decay of $\phi_q^s(t)$, which will especially affect the temperature dependence of the α time scale,[13] and due to the fact that the linear extrapolation for the α time scale is based on a small temperature interval far away from the resulting T_c value, the critical temperature determined from the β time scale and from the amplitude of the scaling function seems to be more reliable than that from (14).

Equipped with these results one can still perform several cross checks. One possible cross check consists in combining the fitted values for the amplitude of the scaling function and the β time scale in such a way that it is again possible to estimate T_c by a linear extrapolation.

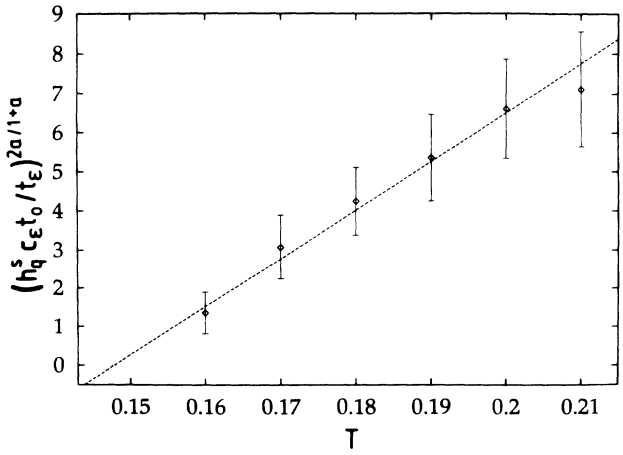

FIG. 15. Cross check based on Eqs. (9) and (10). A plot of $\left(h_q^s c_\epsilon t_0/t_\epsilon\right)^{2a/1+a}$ vs temperature should yield a straight line, which crosses zero at T_c. The diamonds correspond to the results obtained from Table I and the dashed line is again a least-squares fit, giving a critical temperature of $T_c = 0.148$.

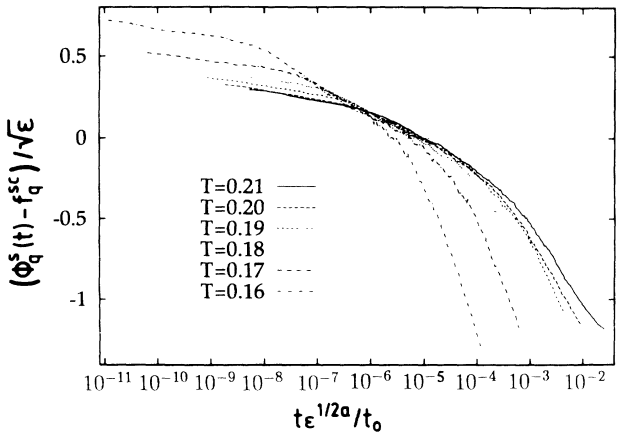

FIG. 16. Crosscheck based on the scaling property of the β regime. In a plot of $h_q^s g\,(t/t_\epsilon)$ vs t/t_ϵ the simulation data for all temperatures should fall on one curve as long as the idealized theory describes the decay of $\phi_q^s(t)$. This expectation is fulfilled for $T \geq 0.19$, whereas (4) does not succeed in scaling the smaller temperatures.

A glance at the Eqs. (9) and (10) shows that the combination $\left(h_q^s c_\epsilon t_0/t_\epsilon\right)^{2a/1+a}$ should linearly depend upon temperature and become zero at T_c. Figure 15 reveals that this expectation is fulfilled, yielding a critical temperature $T_c = 0.148^{+0.004}_{-0.006}$, which compares very well with the values obtained from $h_q^s c_\epsilon$ and t_ϵ directly. In another cross check one can try to test the scaling property of the β regime by plotting $h_q^s g\,(t/t_\epsilon) = [\phi_q^s(t) - f_q^{sc}]/c_\epsilon$ versus the reduced time t/t_ϵ using $T_c = 0.150$ and the values compiled in (18). If the scaling property applied, all data should collapse on a temperature-independent master curve in the β-relaxation regime. Figure 16 shows that this is only the case for the temperatures larger than $T = 0.19$, whereas (6) and (7) are not the adequate expansions of the scaling function for $T < 0.19$.

V. SUMMARY AND OUTLOOK

In this paper we calculated the incoherent intermediate scattering function $\phi_q^s(t)$ during a Monte Carlo simulation for a dense polymer melt by using a coarse-grained lattice model, the bond-fluctuation model, which has the advantage that one can obtain good statistics and cover six to seven decades in the significant time window. Good statistics are necessary if one attempts to analyze the line shape of $\phi_q^s(t)$ quantitatively, whereas long simulation times are also required in order to account for the major theoretical precondition of thermal equilibrium in the important temperature region as much as possible. In the temperature interval $T \in [0.16, 0.21]$ (Ref. 40) we tried to fit $\phi_q^s(t)$ by the asymptotic expression of the idealized MCT. This analysis splitted the considered temperature interval in two parts. In the high-temperature part ($T \geq 0.19$) the idealized MCT accurately describes the decay of $\phi_q^s(t)$ in the β regime over about three decades in time, yielding a very good matching with both the expansion of $\phi_q^s(t)$ within the Rouse model for short times and the Kohlrausch law for the long times of the α process.

However, in the low-temperature region ($T < 0.19$) the idealized theory only accounts for the initial decay of the correlator, whereas it overestimates the freezing tendency of the melt the longer the time and the smaller the temperature become. This observation for $T < 0.19$ can be rationalized theoretically by including hopping processes in the theory, which restore ergodicity for all temperatures and thus dominate the dynamics in the immediate vicinity of the critical point. In this extended version of the MCT the subtle interplay between the cage effect and the hopping processes close to T_c leads to a complicated relaxation scenario in which the idealized theory can only account for the initial decay of the correlators. Therefore, the simulation results are qualitatively in agreement with the predictions of the extended MCT. If one extracts the critical temperature from the fit with idealized theory one can estimate an upper bound for the δ term by virtue of Eq. (13). Combining the results of the fit with the expansion of the β correlator one obtains $T_c \approx 0.150$, and thus the ε values, where the idealized theory applies in this simulation, typically range between $\varepsilon = 0.4$ for $T = 0.21$ and $\varepsilon = 0.2\bar{6}$ for $T = 0.19$. Although these ε values are compatible with those found in experiments[20,21,48] they are distinctly larger than the typical distances to T_c in second-order phase transitions, where $\varepsilon < 0.1$ or even $\varepsilon < 0.01$ is required to extract the asymptotic power laws correctly.[49] Although the critical behavior of the idealized MCT has a completely different origin than that of second-order phase transitions, the wide extent of ε, over which one can observe the influence of the dynamic singularity in this simulation in comparison to the tiny region around T_c which one must enter in order to feel the singularity of a phase transition, raises some questions about the significance of the idealized MCT for our model. Since the idealized theory departs from the simulation data for $T \leq 0.18$, $T = 0.18$ may be used as an estimate for ε_0 so that the upper bound of the hopping term a value of $\delta t_0 \approx 7 \times 10^{-3}$, a value which is much higher than that found in a recent application of the extended theory.[48] Whether reasonable $\delta(T)$ data will actually succeed in resolving the left discrepancies between the simulation results and the idealized theory is an interesting problem for future work.

In summary, we have presented very extensive and statistically accurate simulation data for the incoherent scattering function of a simple model for a polymer melt undergoing a glass transition. While these data have been used to test the idealized MCT one must realize that this theory contains a number of adjustable parameters, and presumably the extended theory, which takes the hopping processes into account, will involve even more parameters. The question of understanding these parameters from the microscopic model Hamiltonian, which is well specified in this simulation, has not been addressed here but will be a challenging problem for the future. At the same time, the simulation yields detailed information on many other quantities (temperature dependence of effective bond lengths, bond angles, chain radii, various types of relaxation functions and associated relaxation times, etc.), some of which have been analyzed in previous papers.[37,38,50] It is a challenging task to develop a theoretical framework that can explain the wealth of these simulation data in a coherent way.

ACKNOWLEDGMENTS

I am very grateful to the Höchstleistungsrechenzentrum (HLRZ) at Jülich for a generous grant of computer time on the CRAY YMP and to the Deutsche Forschungsgemeinschaft for support of this work under Grant No. SFB 262. Special thanks go to Professor K. Binder and W. Paul for many helpful discussions during all stages of this work as well as to E. Bartsch for pointing out Ref. 45 to me and for informing me about his analysis prior to publication. I am also indebted to Professor W. Götze for his critical comments and valuable suggestions, which have very much influenced the final form of this paper.

[1] J. Jäckle, Rep. Prog. Phys. **49**, 171 (1986).
[2] R. Zallen, *The Physics of Amorphous Solids* (Wiley, New York, 1983).
[3] J. P. Hansen and I. R. McDonald, *Theory of Simple Liquids* (Academic, New York, 1986).
[4] J. P. Boon and S. Yip, *Molecular Hydrodynamics* (McGraw-Hill, New York, 1980).
[5] J. Wong and C. A. Angell, *Glass: Structure by Spectroscopy* (Dekker, Basel, 1976).
[6] S. Brawer, *Relaxation in Viscous Liquids and Glasses* (The American Ceramics Society, Columbus, OH, 1985).
[7] C. A. Angell and W. Sichina, Ann. N.Y. Acad. Sci. **279**, 53 (1976); C. A. Angell, J. Phys. Chem. **49**, 863 (1988); J. Non-Cryst. Solids **191**, 13 (1991).
[8] T. A. Vilgis, Phys. Rev. B **47**, 2882 (1993).
[9] W. Götze, in *Liquids, Freezing and the Glass Transition*, edited by J. P. Hansen, D. Levesque, and J. Zinn-Justin (North-Holland, Amsterdam, 1990).
[10] W. Götze and L. Sjögren, Rep. Prog. Phys. **55**, 241 (1992).
[11] R. Schilling, in *Disorder Effects on Relaxational Processes*, edited by R. Richert and A. Blumen (Springer, Heidelberg, in press).
[12] R. G. Palmer, Adv. Phys. **31**, 669 (1982).
[13] M. Fuchs, W. Götze, S. Hildebrand, and A. Latz, J. Phys.: Condens. Matter **4**, 7709 (1992).
[14] W. van Megen and P. N. Pusey, Phys. Rev. A **43**, 5429 (1991); Phys. Rev. Lett. **67**, 1586 (1991).
[15] E. Bartsch, H. Bertagnolli, P. Chieux, A. David, and H. Sillescu, Chem. Phys. **169**, 373 (1993).
[16] B. Frick, D. Richter, and Cl. Ritter, Europhys. Lett. **9**, 557 (1989).
[17] M. Elmroth, L. Börjesson, and L. M. Torell, Phys. Rev. Lett. **68**, 79 (1992).
[18] W. Petry, E. Bartsch, F. Fujara, M. Kiebel, H. Sillescu, and B. Farago, Z. Phys. B **83**, 175 (1991).
[19] F. Mezei, W. Knaak, and B. Farago, Phys. Rev. Lett. **58**, 571 (1987); W. Knaak, F. Mezei, and B. Farago, Europhys. Lett. **7**, 529 (1988).
[20] G. Li, W. M. Du, X. K. Chen, H. Z. Cummins, and N. J. Tao, Phys. Rev. A **45**, 3867 (1992).

[21] E. Bartsch, M. Antonietti, W. Schupp, and H. Sillescu, J. Chem. Phys. **97**, 3950 (1992).
[22] B. Frick, D. Richter, W. Petry, and U. Buchenau, Z. Phys. B **70**, 73 (1988); B. Frick, B. Farago, and D. Richter, Phys. Rev. Lett. **64**, 2921 (1990).
[23] W. Doster, S. Cusack, and W. Petry, Phys. Rev. Lett. **65**, 1080 (1990).
[24] G. Wahnström, J. Non-Cryst. Solids **131-133**, 109 (1991).
[25] G. Wahnström, Phys. Rev. A **44**, 3752 (1991).
[26] H. Loewen, J. P. Hansen, and J.-N. Roux, Phys. Rev. A **44**, 1169 (1991); G. Szamel and H. Löwen, *ibid.* **44**, 8215 (1991).
[27] W. Kob, and H. C. Andersen, Phys. Rev. E **47**, 4210 (1993).
[28] J. L. Barrat, W. Götze, and A. Latz, J. Phys.: Condens. Matter **1**, 7163 (1989); J. N. Roux, J. L. Barrat, and J.-P. Hansen, *ibid.* **1**, 7171 (1989).
[29] W. Paul, in *Slow Dynamics in Condensed Matter, Fukuoka, Japan, 1991*, edited by K. Kawasaki, M. Tokuyama, and T. Kawakatsu, AIP Conf. Proc. No. 256 (AIP, New York, 1992), p. 145.
[30] G. F. Signorini, J. L. Barrat, and M. L. Klein, J. Chem. Phys. **92**, 1294 (1990).
[31] R. Richert and H. Bässler, J. Phys.: Condens. Matter **2**, 2273 (1990); L. Sjögren, in *Basic Features of the Glassy State*, edited by J. Colmenero and A. Alegria (World Scientific, Singapore, 1990); J. Phys.: Condens. Matter **3**, 5023 (1991); L. Sjögren and W. Götze, J. Non-Cryst. Solids **131-133**, 153 (1991); W. Götze, in *Vth International Symposium on Selected Topics in Statistical Mechanics*, edited by A. A. Logunov, N. N. Bogolubov, Jr., V. G. Kadyshevsky, and A. S. Shumovsky (World Scientific, Singapore, 1990); W. Götze and L. Sjögren, J. Non-Cryst. Solids **131-133**, 161 (1991).
[32] M. Fuchs, W. Götze, I. Hofacker, and A. Latz, J. Phys.: Condens. Matter **3**, 5047 (1991).
[33] P. J. Flory, *Statistical Mechanics of Chain Molecules* (Wiley, New York, 1969).
[34] I. Carmesin and K. Kremer, Macromolecules **21**, 2819 (1988).
[35] H.-P. Deutsch and K. Binder, J. Chem. Phys. **94**, 2294 (1991).
[36] H.-P. Wittmann and K. Kremer, Comput. Phys. Commun. **61**, 309 (1990); **71**, 343 (1992).
[37] J. Baschnagel, K. Binder, and H.-P. Wittmann, J. Phys. C **5**, 1597 (1993).
[38] J. Baschnagel and K. Binder, Physica A (to be published).
[39] K. Kremer and K. Binder, Comput. Phys. Rep. **7**, 259 (1988).
[40] The temperature is measured in units of an energy parameter introduced in the Hamiltonian. All lengths are measured in units of the lattice constant.
[41] J. Baschnagel, H.-P. Wittmann, W. Paul, and K. Binder, in *Trends in Non-Crystalline Solids*, edited by A. Conde, C. F. Conde, and M. Millán (World Scientific, Singapore, 1992).
[42] J. Baschnagel, K. Binder, W. Paul, M. Laso, U. W. Suter, I. Batoulis, W. Jilge, and T. Bürger, J. Chem. Phys. **95**, 6014 (1991).
[43] J. Baschnagel, K. Qin, W. Paul, and K. Binder, Macromolecules **25**, 3117 (1992).
[44] M. Doi and S. F. Edwards, *Theory of Polymer Dynamics* (Clarendon, Oxford, 1986).
[45] W. Götze, J. Phys.: Condens. Matter **2**, 8485 (1990).
[46] A. Baumgärtner and K. Binder, J. Chem. Phys. **75**, 2994 (1981).
[47] W. Paul, K. Binder, D. W. Heermann, and K. Kremer, J. Phys. II **1**, 37 (1991).
[48] H. Z. Cummins, W. M. Du, M. Fuchs, W. Götze, S. Hildebrand, A. Latz, G. Li, and N. J. Tao, Phys. Rev. E **47**, 4223 (1993).
[49] P. Heller, Rep. Prog. Phys. **30**, 731 (1967); H. E. Stanley, *An Introduction to Phase Transitions and Critical Phenomena* (Oxford University Press, Oxford, 1971).
[50] H.-P. Wittmann, K. Kremer, and K. Binder, J. Chem. Phys. **96**, 6291 (1992); Makromolek. Chem. Theor. Simulations **1**, 275 (1992).